NEW THREE AND FOUR NODED PLATE BENDING ELEMENTS

Mikko Lyly and Rolf Stenberg

Summary. We report on calculations with two new low-order Reissner-Mindlin plate bending elements obtained by combining a recent stabilization technique with a mixed interpolation of shear strains. The methods are a stabilization of a linear triangular element by Hughes and Taylor and a stabilization of the bilinear quadrilateral method MITC4 by Bathe and Dvorkin.

Introduction

Recently considerable progress has been made in the construction of good finite element methods for "thick" plates with shear deformation. Of the new methods the "MITC" elements (Mixed Interpolated Tensorial Components), introduced by Bathe and Dvorkin, have been among the most succesful. They have been reported to performed excellently in numerous test calculations, cf. [9, 10, 11]. It has also been possible to give a mathematical error analysis of these methods, cf. [7, 8] for the analysis in the limiting "Kirchhoff" case and [13] where a complete error analysis is given. The analysis shows that the methods are stable and of optimal accuracy if the polynomial order of the methods are at least two.

The bilinear quadrilateral element of this type, the MITC4, is not stable. Nevertheless, it is known to work quite well in practical calculations. In our recent computational paper [24] we, however, showed that there are cases when the accuracy decreases due to the lack of stability.

The linear triangular element that one obtains from the MITC family is an element that was introduced by Hughes and Taylor [21] (henceforth abbreviated HT). In their paper it was reported that the element performs well for certain mesh configurations but badly for others. Hence, the method does not seem to be reliable enough to be used in practice. From a theoretical standpoint the irregular behaviour is expected since the method is not stable.

In [13] we, however, showed that both the HT and MITC4 elements can easily be modified to get elements which are stable and of optimal accuracy. The idea was to combine the elements with a stabilization technique originally introduced by Fried and Yang [18]. Recently this technique has been mathematically analyzed and also generalized in several ways, cf. [26, 20, 28].

We should mention that in addition to the elements considered in this paper we know of only two linear elements for which the convergence have been rigorously proved; an element by Arnold and Falk [2], and a MITC-type element, mentioned in [13, page 145] and independently introduced by Durán and Liberman [15]. In [17] it was shown that the stabilization technique of Fried and Yang can also be applied to simplify the Arnold-Falk element. These elements are of the same order of accuracy as the elements considered here, but for the same mesh they lead to a greater number of degrees of freedom. Hence, the present elements seem to be preferable. We should, however, mention that both the original and modified Arnold-Falk elements work well in practice, cf. [16, 29] where some computational results are presented.

The purpose of this paper is to present the results of some test calculations with the stabilized HT and MITC4 elements. We also compare with the results obtained with the corresponding unstabilized elements and also the "classical" bilinear element with selectively reduced integration. For the quadrilateral elements calculations of this type have recently been presented in our paper [24]. Here we complement this paper by giving the results for other test problems. Computational results for the triangular element have earlier only been presented in the conference paper [29]. Here we also present the elements using a notation which might be easier when considering a computer implementation.

Thick plate theory

Let Ω be the region occupied of the plate and denote by $w(x,y)$ and $\beta(x,y) = (\beta_x \ \beta_y)^T$ the transverse deflection and the rotations of the normal of the plate, respectively. With the given load f the solution to the plate bending problem is then obtained by minimizing the total potential energy, i.e. it holds [32]

$$\Pi(w,\beta) = \min_{(v,\eta)} \Pi(v,\eta), \tag{1}$$

with

$$\Pi(v,\eta) = \frac{1}{2}\int_\Omega (L\eta)^T E L\eta \, d\Omega + \frac{1}{2}\int_\Omega (\nabla v - \eta)^T G (\nabla v - \eta) \, d\Omega - \int_\Omega f v \, d\Omega. \tag{2}$$

The minimization is performed in the set of all kinematically admissible deflections and rotations for which the strain energy is finite. For simplicity, we have assumed

4

that no shear force nor bending moment has been prescribed on the free boundary. L is the "curvature" operator for vector valued functions and ∇ is the usual gradient operator for scalar functions, viz.

$$L = \begin{pmatrix} \partial/\partial x & 0 \\ 0 & \partial/\partial y \\ \partial/\partial y & \partial/\partial x \end{pmatrix}, \qquad \nabla = \begin{pmatrix} \partial/\partial x \\ \partial/\partial y \end{pmatrix}. \tag{3}$$

E and G are the elasticity matrices for the bending and for the shear, respectively. For the isotropic linear elastic materials we have

$$E = \frac{Et^3}{12(1-\nu^2)} \begin{pmatrix} 1 & \nu & 0 \\ \nu & 1 & 0 \\ 0 & 0 & \frac{1-\nu}{2} \end{pmatrix}, \qquad G = \frac{E\kappa t}{2(1+\nu)} \begin{pmatrix} 1 & 0 \\ 0 & 1 \end{pmatrix}, \tag{4}$$

where E is the Young modulus and ν is the Poisson ratio. t denotes the thickness of the plate (assumed constant) and κ is the shear correction factor which usually takes the value 5/6.

The bending moments $M(x, y)$ and the shear forces $Q(x, y)$ are obtained from the solution w and β through the equations

$$M = \left(M_x \ M_y \ M_{xy} \right)^T = E \, L\beta, \tag{5}$$

$$Q = \left(Q_x \ Q_y \right)^T = G \left(\nabla w - \beta \right). \tag{6}$$

The shear strain is given by

$$\gamma = \nabla w - \beta. \tag{7}$$

The finite element methods

The Hughes-Taylor and Bathe-Dvorkin elements

The method by Hughes and Taylor [21] is a triangular element using the standard linear basis functions for the deflection and the rotation. In the quadrilateral method of Bathe and Dvorkin [11], the MITC4, isoparametric bilinear basis functions are used. Hence, we can use the established notation [31]

$$w_{FE} = N_w \bar{w}, \tag{8}$$

$$\beta_{FE} = N_\beta \bar{\beta}, \tag{9}$$

where $\bar{w}$ and $\bar{\beta}$ stand for the nodal values of w_{FE} and β_{FE}, respectively. $N_w(x, y)$ and $N_\beta(x, y)$ are the usual shape function matrices for the three (HT) or four (MITC4) noded elements.

For the shear strain different basis functions are used. Let (ξ, η) be the coordinates of the reference element Ω^{ref} and let

$$J_e = \begin{pmatrix} \partial x/\partial\xi & \partial y/\partial\xi \\ \partial x/\partial\eta & \partial y/\partial\eta \end{pmatrix} \tag{10}$$

be the Jacobian matrix of the mapping from Ω^{ref} to the element Ω^e. On the element Ω^e the shear strain is approximated by functions of the form

$$\gamma_e = J_e^{-1}\gamma_e^{ref}, \tag{11}$$

with

$$\gamma_e^{ref} = \begin{pmatrix} a_e - c_e\eta \\ b_e + c_e\xi \end{pmatrix} \quad \text{for HT,} \tag{12}$$

$$\gamma_e^{ref} = \begin{pmatrix} a_e + c_e\eta \\ b_e + d_e\xi \end{pmatrix} \quad \text{for MITC4.} \tag{13}$$

The local degrees of freedom are given by the parameters a_e, b_e, c_e and d_e (for the MITC4).

Now, along the edges of reference element the tangential component of the shear strain is a constant (i.e. independent of ξ and η). By the definition (11) this also holds on the final element; $\tau^T\gamma_e$ is a constant, independent of x and y, on each edge of the element, where $\tau = (\tau_x\ \tau_y)^T$ is the tangent to the edge. (We should here also remark that for the HT element γ_e^{ref} consists of the rigid body motions on Ω^{ref}. It is quite easily seen that this property is preserved by the mapping; on Ω^e also γ_e consists of the rigid body motions.) With this local representation we are now able to define the global basis functions for the shear so that the tangential component is continuous across inter element boundaries. As the degrees of freedom we take the tangential component at the midpoints of each edge.

Let us denote the shear strain approximation so obtained as

$$\gamma_{FE} = N_\gamma\bar{\gamma}. \tag{14}$$

The shear strain $\nabla w_{FE} - \beta_{FE}$ obtained from the representations (8) and (9) is now interpolated with these new basis functions. Hence, we define γ_{FE} from the condition that

$$\tau^T\gamma_{FE} = \tau^T\left(\nabla w_{FE} - \beta_{FE}\right), \tag{15}$$

in the midpoints of the edges to the element. Now, since it holds (cf. [31])

$$\nabla N_w(x, y) = J_e^{-1}\nabla N_w(\xi, \eta) \quad \text{on the element } \Omega^e, \tag{16}$$

4

and since $\tau^T \nabla w_{FE}$ is constant and continuous along interelement edges, we conclude that ∇w_{FE} can be exactly represented by the basis functions for the shear. Hence, the condition (15) means that modified basis functions, denoted by $\tilde{N}_\beta$, are used in the shear expression, viz.

$$\gamma_{FE} = \nabla N_w \bar{w} - \tilde{N}_\beta \bar{\beta}. \tag{17}$$

In the finite element methods this modified shear expression is used. Hence, we seek the the solution from the minimizing condition

$$\Pi_{FE}(\bar{w}, \bar{\beta}) = \min_{(\bar{v}, \bar{\eta})} \Pi_{FE}(\bar{v}, \bar{\eta}) \tag{18}$$

with the finite element energy defined as

$$\begin{aligned} \Pi_{FE}(\bar{v}, \bar{\eta}) &= \frac{1}{2} \int_\Omega (L N_\beta \bar{\eta})^T E\, L N_\beta \bar{\eta}\, d\Omega \\ &\quad + \frac{1}{2} \int_\Omega (\nabla N_w \bar{v} - \tilde{N}_\beta \bar{\eta})^T G (\nabla N_w \bar{v} - \tilde{N}_\beta \bar{\eta})\, d\Omega - \int_\Omega f v\, d\Omega. \end{aligned} \tag{19}$$

This leads to the system of equations

$$\begin{pmatrix} k_{ww} & k_{w\beta} \\ k_{w\beta}^T & k_{\beta\beta} \end{pmatrix} \begin{pmatrix} \bar{w} \\ \bar{\beta} \end{pmatrix} = \begin{pmatrix} f \\ 0 \end{pmatrix}, \tag{20}$$

where f is the force vector, given elementwise through

$$f^e = \int_{\Omega^e} f N_w^T\, d\Omega. \tag{21}$$

The element stiffness matrix is given by

$$k_{ww}^e = \int_{\Omega^e} (\nabla N_w)^T G \nabla N_w\, d\Omega, \tag{22}$$

$$k_{w\beta}^e = -\int_{\Omega^e} (\nabla N_w)^T G \tilde{N}_\beta\, d\Omega, \tag{23}$$

$$k_{\beta\beta}^e = \int_{\Omega^e} \tilde{N}_\beta^T G \tilde{N}_\beta\, d\Omega + \int_{\Omega^e} (L N_\beta)^T E\, L N_\beta\, d\Omega. \tag{24}$$

The approximate shear force is obtained from

$$Q_{FE} = G (\nabla N_w \bar{w} - \tilde{N}_\beta \bar{\beta}). \tag{25}$$

In Figure 1 we show the degrees of freedom for the HT and MITC4 elements. We would like to repeat that the degrees of freedom for the shear do not enter into the calculations. They are only used in the construction of the stiffness matrix.
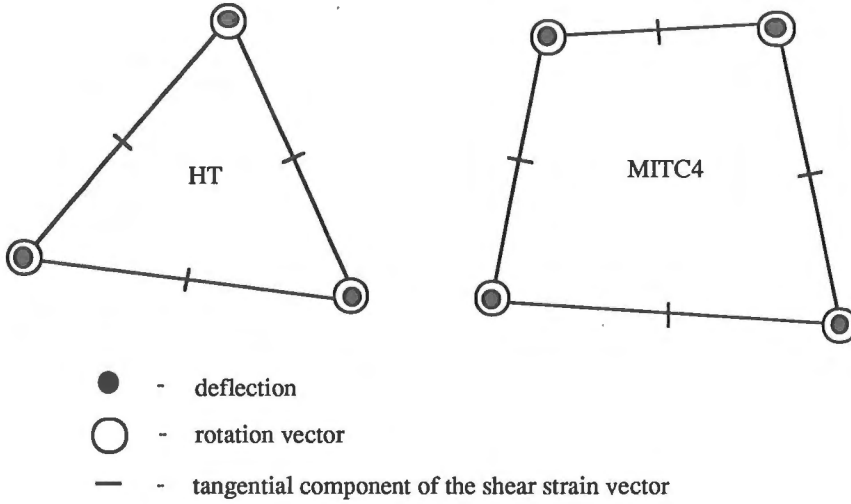
Figure 1: Degrees of freedom for the HT and MITC4 elements and their stabilized modifications.

The Hughes-Taylor element with reduced integration

In [21] it was shown that the HT element performs better if the energy expression is calculated inexactly with the midpoint rule. The method obtained is then given by (20) with

$$k_{ww}^e = (\nabla N_w(x_e, y_e))^T G \, \nabla N_w(x_e, y_e) \, A_e, \tag{26}$$

$$k_{w\beta}^e = -(\nabla N_w(x_e, y_e))^T G \, \tilde{N}_\beta(x_e, y_e) \, A_e, \tag{27}$$

$$k_{\beta\beta}^e = \tilde{N}_\beta(x_e, y_e)^T G \, \tilde{N}_\beta(x_e, y_e) \, A_e + (LN_\beta(x_e, y_e))^T E \, LN_\beta(x_e, y_e) \, A_e, \tag{28}$$

where (x_e, y_e) is the midpoint of the element Ω^e and A_e is its area. We remark that the bending energy is still evaluated exactly by this. The shear force is piecewise constant given by

$$Q_{FE} = G \left(\nabla N_w(x_e, y_e) \bar{w} - \tilde{N}_\beta(x_e, y_e) \, \bar{\beta} \right) \quad \text{on the element } \Omega^e. \tag{29}$$

The stabilized Hughes-Taylor and Bathe-Dvorkin elements [13, 24]

The stabilized methods are obtained in a very simple way, in the discrete energy expression (19) the shear elasticity matrix G is replaced with the following modification

$$G_{FE} = \left(\frac{t^2}{t^2 + \alpha h_e^2} \right) G \quad \text{on the element } \Omega^e. \tag{30}$$

8

Here h_e is the length of the diameter of the element Ω^e and α is a positive parameter. The stiffness matrix obtained is as in (20) with

$$k^e_{ww} = \int_{\Omega^e} (\nabla N_w)^T G_{FE} \nabla N_w \, d\Omega, \tag{31}$$

$$k^e_{w\beta} = -\int_{\Omega^e} (\nabla N_w)^T G_{FE} \tilde{N}_\beta \, d\Omega, \tag{32}$$

$$k^e_{\beta\beta} = \int_{\Omega^e} \tilde{N}_\beta^T G_{FE} \tilde{N}_\beta \, d\Omega + \int_{\Omega^e} (LN_\beta)^T E \, LN_\beta \, d\Omega. \tag{33}$$

With $\alpha = 0$ we recover the original elements. Note also that when the mesh size approach zero the modified methods converge towards the original ones.

The shear force is given by (note that G_{FE} varies from element to element)

$$Q_{FE} = G_{FE}(\nabla N_w \bar{w} - \tilde{N}_\beta \bar{\beta}) \quad \text{on the element } \Omega^e. \tag{34}$$

The quadrilateral method with selective reduced integration [19]

In the quadrilateral method with selective reduced integration an inexact midpoint integration rule is used for the shear term. Hence, the stiffness matrix of the method is as in (20) with

$$k^e_{ww} = (\nabla N_w(x_e, y_e))^T G \nabla N_w(x_e, y_e) A_e, \tag{35}$$

$$k^e_{w\beta} = -(\nabla N_w(x_e, y_e))^T G N_\beta(x_e, y_e) A_e, \tag{36}$$

$$k^e_{\beta\beta} = N_\beta(x_e, y_e)^T G N_\beta(x_e, y_e) A_e + \int_{\Omega^e} (LN_\beta)^T E \, LN_\beta \, d\Omega, \tag{37}$$

where again (x_e, y_e) and A_e are the midpoint and the area of Ω^e, respectively.

The shear force is given by

$$Q_{FE} = G \left(\nabla N_w \bar{w}(x_e, y_e) - N_\beta \bar{\beta}(x_e, y_e) \right) \quad \text{on the element } \Omega^e. \tag{38}$$

Error estimates for the methods

In this section we will review the known theoretical results with respect to the convergence of the methods. When studying the convergence and locking, one has to consider a sequence of problems for which the load varies as $f = t^3 g$ with the function g fixed. With this the exact solution to (1) has a nonvanishing and finite limit when $t \to 0$. For a well designed locking-free element the convergence should be independent of the plate thickness t for this sequence of problems. The error

estimates proved for finite element methods are usually given in "L_2-norms", i.e. the norms defined by (cf. [31, page 401])

$$
\begin{cases}
\|v\|_{L_2} = [\int_\Omega \ v^2 \ d\Omega]^{1/2}, & \text{for scalar functions,} \\
\\
\|\eta\|_{L_2} = [\int_\Omega \eta^T \eta \ d\Omega]^{1/2} & \text{for vector valued functions.}
\end{cases}
\tag{39}
$$

The error estimates are given with the mesh parameter (cf. [19, 31])

$$
h = \max_{1 \le e \le N_{el}} h_e.
\tag{40}
$$

For the MITC4 it is possible to prove error estimates for a particular class of meshes for which the region is first divided into quadrilateral subregions and then every subregion is regularly divided into quadrilaterals (we refer to [27] for the exact statement of this). For this class of meshes it has been possible to prove that [7, 8, 13]

$$
\|M - M_{FE}\|_{L_2} \le Ch,
\tag{41}
$$

and

$$
\|\nabla w - \nabla w_{FE}\|_{L_2} \le Ch.
\tag{42}
$$

For the case when the elements are rectanguar it additionally holds [7, 8]

$$
\|w - w_{FE}\|_{L_2} \le Ch^2.
\tag{43}
$$

Here C denotes different positive constants which only depend on the exact solution to the problem. The constants are independent of the plate thickness t which means that the method will not lock (for this particular class of meshes). We remark that for a method that locks, the usual error analysis would lead to estimates as above with $C \to \infty$, when $t \to 0$. For the above estimates to be valid it is required that the L_2-norm of all second partial derivatives of the deflection and the rotation are bounded.

In the error analysis the estimates are given for the scaled shear force $q = t^{-3}Q$ since it is this quantity that has a finite non-vanishing limit when $t \to 0$ (with the above scaling of the load). For this quantity the best estimate obtained is (this estimate can be derived by combining results from [13, 22, 27]) (below c will denote different positive constants)

$$
\|q - q_{FE}\|_{L_2} \le C \left(\frac{h}{t + ch^2} \right),
\tag{44}
$$

We see that for very thin plates the shear obtained with the MITC4 may be highly unreliable. That this is the case we will show by our numerical examples.

For the HT element (with both exact and reduced integration) there has not been presented any error estimates. In fact, an attempt to perform an analysis reveals that the element cannot be very good. That this is the case will be shown in the next section.

For the stabilized MITC4 and HT a complete error analysis can be given, cf. [13]. The methods will converge optimally, the estimates (41) and (42) hold for general finite element meshes. For the shear the following estimate is derived, which also is optimal,

$$\|q - q_{FE}\|_{L_2} \leq C \left(\frac{h}{t+h} \right). \tag{45}$$

We see that the shear does not necessarily have to converge, but it stays bounded independent of the plate thickness.

For the quadrilateral method with selective reduced integration an error analysis was presented in [22]. They proved both the estimates (41) and (42) but under very restrictive conditions; the elements have to be rectangular and much more smoothness is required of the exact solution. The estimate for the shear they obtained is

$$\|q - q_{FE}\|_{L_2} \leq C \left(\frac{h}{t + ch^3} \right). \tag{46}$$

Hence, the shear obtained with that method cannot, in general, be very good.

Numerical results

We perform all our numerical tests for one geometrical configuration, a square plate of unit side length occupying the region $\Omega = [0,1] \times [0,1]$. In all cases the loading and boundary conditions will be symmetric so that only one quarter of the plate will be analyzed. The physical parameters are chosen as $E = 1$ and $\nu = 0.3$. For the shear correction factor we take the usual value[1] $\kappa = 5/6$. The stability parameter is taken as $\alpha = 0.1$ for the stabilized MITC4 and $\alpha = 0.2$ for the stabilized HT.

Convergence studies for regular and irregular meshes

In the first test case the plate is subject to a uniform load acting on the area $[3/8, 5/8] \times [3/8, 5/8]$. As the boundary conditions we choose the "hard" simply supported case, i.e. both the deflection and the tangential component of the rotation vanish on the boundary. With this choice all the variables of interest converge

---

[1]Below we will show that the stabilized methods are the methods that work best. In those the shear term is modified quite much, and hence the value of the shear correction factor seems to be a rather irrelevant question.
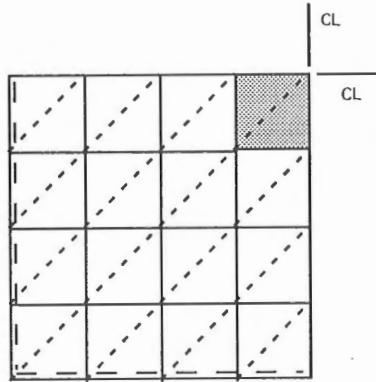
Figure 2: One symmetric quarter of the simply supported test plate. The plate is subject to a pressure load acting on the dotted area.

in the L_2-norm towards the classical Kirchhoff solution when $t \to 0$. It should here be pointed out that for the "soft" simply supported case when only the deflection vanish on the boundary, the shear obtained from the Reissner-Mindlin model does not converge in the L_2-norm towards the Kirchhoff solution, cf. [1, 3] and [12, page 408] for a numerical example.

When testing a plate element for locking the most revealing is to do it for thin plates. This we will do and due to the boundary conditions chosen we can consider the Kirchhoff solution as the exact one. This we calculate with classical series techniques [25].

The quadrilateral partitioning is obtained by dividing the quarter plate into $N \times N$ equal squares as shown in Figure 2. The triangulation is then obtained by drawing in each square the diagonal from the bottom left to the top right corner. This triangulation is the one for which the Hughes-Taylor elements were reported to perform best in their article [21].

We also repeat the calculations for a sequence of irregular meshes obtained by moving each node by random in the neighborhood of its original position as shown in Figure 3. The nodes lying on the boundary of the loading area are naturally not moved.

We first choose $t = 0.01$ and then calculate the normalized center point deflection and the L_2-errors for the deflection, bending moment and shear force using the different elements. The results are shown in Tables 1 - 8. (The stabilized HT is denoted by STAB3, the stabilized modification of the MITC4 element is referred to as STAB4 and the HT element with reduced integration (for the shear energy)
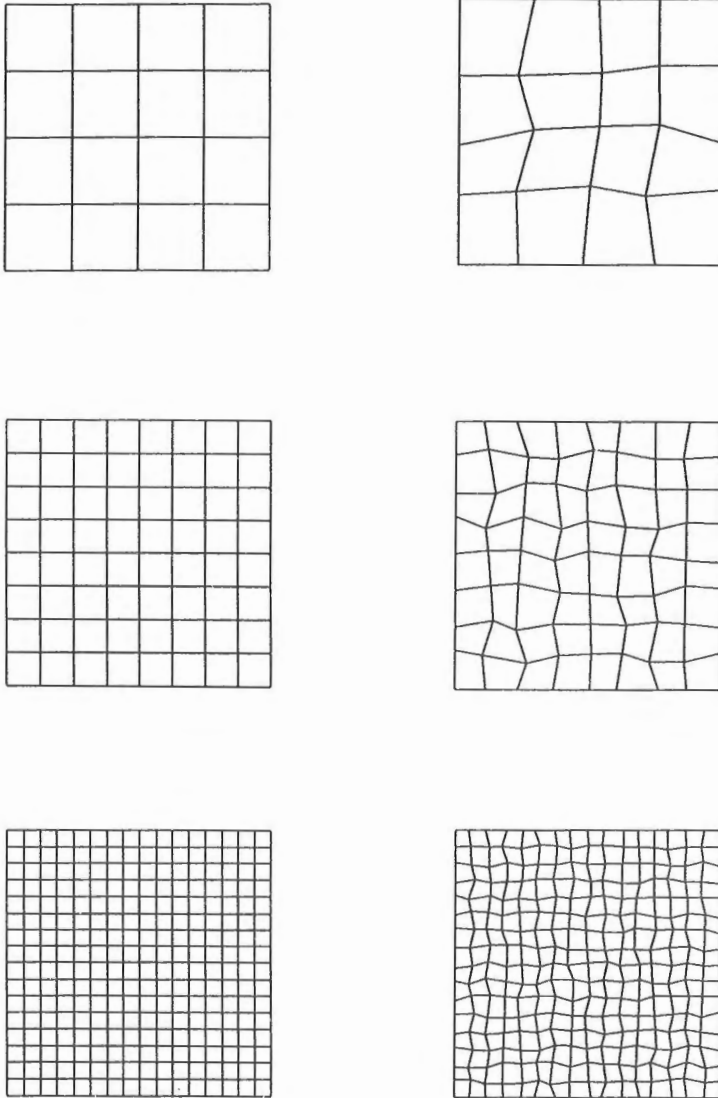
Figure 3: Examples of the finite element meshes. The triangular elements are obtained by splitting each quadrilateral element by drawing a straight line from its bottom left corner to the top right corner.

is abbreviated as HTRI).

In Tables 3 and 4, INT denotes the Lagrange interpolant for the deflection (i.e. a finite element deflection with exact nodal values). In Tables 5 and 6, INT means, however, the bending moment calculated from the Lagrange interpolant for the rotation. The normalized L_2-errors for the interpolants are shown in order to approximately define the "best possible level" for the results obtained by using the finite elements - if the interpolant is bad then there is no reason to expect a good finite element solution either.

Table 1. The normalized centerpoint deflections $w_{FE}(\text{center})/w(\text{center})$ for the regular and irregular meshes with $t = 0.01$. Three noded elements.

| | STAB3 | | HT | | HTRI | |
N	Regular	Irregular	Regular	Irregular	Regular	Irregular
4	0.9670	0.9648	0.6910	0.6713	0.8922	0.8816
8	0.9925	0.9916	0.9602	0.9578	0.9801	0.9780
16	0.9988	0.9986	0.9946	0.9942	0.9959	0.9956

Table 2. The normalized centerpoint deflections $w_{FE}(\text{center})/w(\text{center})$ for the regular and irregular meshes with $t = 0.01$. Four noded elements.

| | STAB4 | | MITC4 | | SRI | |
N	Regular	Irregular	Regular	Irregular	Regular	Irregular
4	1.0013	1.0057	0.9758	0.9784	0.9759	0.9452
8	1.0012	1.0012	0.9950	0.9940	0.9950	0.9220
16	1.0009	1.0009	0.9994	0.9991	0.9994	0.9744

Table 3. The L_2-errors $\|w - w_{FE}\|_{L_2}/\|w\|_{L_2}$ for the regular and irregular meshes with $t = 0.01$. Three noded elements.

| | STAB3 | | HT | | HTRI | | INT | |
N	Regular	Irregular	Regular	Irregular	Regular	Irregular	Regular	Irregular
4	0.0503	0.0524	0.3112	0.3327	0.1106	0.1235	0.0249	0.0260
8	0.0123	0.0135	0.0416	0.0424	0.0211	0.0228	0.0063	0.0070
16	0.0026	0.0029	0.0059	0.0064	0.0046	0.0050	0.0016	0.0017

Table 4. The L_2-errors $\|w - w_{FE}\|_{L_2}/\|w\|_{L_2}$ for the regular and irregular meshes with $t = 0.01$. Four noded elements.

	STAB4		MITC4		SRI		INT	
N	Regular	Irregular	Regular	Irregular	Regular	Irregular	Regular	Irregular
4	0.0208	0.0191	0.0372	0.0365	0.0372	0.0719	0.0274	0.0274
8	0.0049	0.0056	0.0090	0.0103	0.0090	0.0863	0.0069	0.0077
16	0.0009	0.0010	0.0018	0.0021	0.0018	0.0262	0.0017	0.0019

As we can see from the tables above, the HT element and its modified version with reduced integration lock severely in the case of the coarsest mesh with $N = 4$. For $N = 8$ and $N = 16$ the results are better, but still much less accurate than those obtained with the stabilized version. For the stabilized method the deflection is optimally convergent and almost as good as the interpolant in each case.

The four noded SRI element gives a very good deflection with regular meshes but the accuracy is completely destroyed when the mesh is distorted; the error in deflection is larger for $N = 8$ than it is for $N = 4$, and for $N = 16$ the L_2-error for the irregular mesh is ten times as big as for the regular mesh. That this happens is clearly a sign of the lack of stability of this method. The original MITC4 does not lock in this benchmark example, but still the accuracy is not as good as for its stabilized modification. The stabilized MITC4 gives here the best approximation (better than the interpolant) for the deflection, even for the irregular and coarse meshes.

Table 5. The L_2-errors $\|M - M_{FE}\|_{L_2}/\|M\|_{L_2}$ for the regular and irregular meshes with $t = 0.01$. Three noded elements.

	STAB3		HT		HTRI		INT	
N	Regular	Irregular	Regular	Irregular	Regular	Irregular	Regular	Irregular
4	0.1997	0.2054	0.3511	0.3814	0.2179	0.2290	0.1923	0.1968
8	0.0987	0.1004	0.1057	0.1129	0.0996	0.1029	0.0975	0.0991
16	0.0490	0.0504	0.0493	0.0514	0.0492	0.0506	0.0490	0.0502

Table 6. The L_2-errors $\|M - M_{FE}\|_{L_2}/\|M\|_{L_2}$ for the regular and irregular meshes with $t = 0.01$. Four noded elements.

	STAB4		MITC4		SRI		INT	
N	Regular	Irregular	Regular	Irregular	Regular	Irregular	Regular	Irregular
4	0.1186	0.1188	0.1187	0.1191	0.1187	0.1807	0.1137	0.1155
8	0.0587	0.0632	0.0587	0.0636	0.0587	0.1746	0.0581	0.0623
16	0.0293	0.0314	0.0293	0.0315	0.0293	0.0787	0.0292	0.0313

Tables 5 and 6 give the calculated results for the bending moment. Also here the stabilized (HT and MITC4) elements give the most accurate approximations. According to the theoretical estimate (41) the bending moment is optimally convergent, also with irregular meshes, and the accuracy is practically equal to that of the interpolant.

The original HT fails here again for the coarsest mesh: for $N = 4$ the error is twice as large as for its stabilized modification. The most interesting result is for the SRI element. Again the distortion of the mesh increases the error considerably.

Both the original MITC4 and the HT with reduced integration give good results for the moment.

Next, we give the results for the normalized L_2-errors in the shear force. From Table 7 we see that the stabilized HT gives a shear force which is of the right order of maginitude and converges, although rather slowly. This is in complete accordance with the theoretical result (45). The original Hughes-Taylor elements yield shears that are extremely erraneous (except for the HTRI with the finest mesh).

In Table 8 the results for the quadrilateral methods are given. We see that both the MITC4 and its stabilized modification converge. This convergence is far better than what could be expected from the theoretical analysis and must be explained as a superconvergence effect. The results for the SRI are very interesting. For the regular mesh the convergence and accuracy is very good, but for the irregular mesh the accuracy is extremely bad.

In the calculations the errors in the shear usually show up as oscillations. In Figure 4 the shear component Q_x is given along the horisontal symmetry line.

Table 7. The L_2-errors $\|Q - Q_{FE}\|_{L_2}/\|Q\|_{L_2}$ for the regular and irregular meshes with $t = 0.01$. Three noded elements.

	STAB3		HT		HTRI	
N	Regular	Irregular	Regular	Irregular	Regular	Irregular
4	0.4253	0.4323	14.689	14.584	5.6177	6.2973
8	0.3597	0.3716	5.2791	5.1639	1.2431	1.4258
16	0.2923	0.3057	1.3877	1.4368	0.2474	0.4183

Table 8. The L_2-errors $\|Q - Q_{FE}\|_{L_2}/\|Q\|_{L_2}$ for the regular and irregular meshes with $t = 0.01$. Four noded elements.

	STAB4		MITC4		SRI	
N	Regular	Irregular	Regular	Irregular	Regular	Irregular
4	0.2493	0.2736	0.2497	0.2961	0.2806	3.0391
8	0.1239	0.1668	0.1240	0.2290	0.1431	7.4700
16	0.0610	0.1162	0.0610	0.1357	0.0713	4.7214

After this, we repeat our calculations with a thinner plate and choose $t = 0.001$. Tables 9 - 16 show the results obtained from the calculations. The conclusions are about the same as before. However, the shortcomings of the HT, HTRI, SRI and MITC4 elements are now much more clearly seen. From Tables 13 and 14 we find that the bending moment is now very bad for the HT and HTRI elements.

Again the behaviour of the SRI should be noted. For the regular meshes the results are excellent, but that cannot be said for the irregular meshes. Still, this element is presented in most of the recent textbooks, cf. [19, pages 327-335], [32, pages 69-76] and [14, pages 325-328]. In these works some shortcomings of this element is pointed out, but it seems that the authors have not been fully aware of how erratically this element can behave.

The only elements which are able to properly approximate the deflection and shear force are the stabilized HT and MITC4 elements, and also the original MITC4. For the MITC4 the shear with the irregular mesh is much less accurate than what is obtained with the stabilized form, but still as good as that of the stabilized HT. We should, however, point out that there are other test cases for which the MITC4 fails more severely for plates of this thickness, cf. [24, Table 8].

In Figure 5 we show the shear distribution along the horisontal symmetry line for this case and the MITC4. We here also show the oscillations appearing in the Q_y component which should vanish identically. For the stabilized methods the results
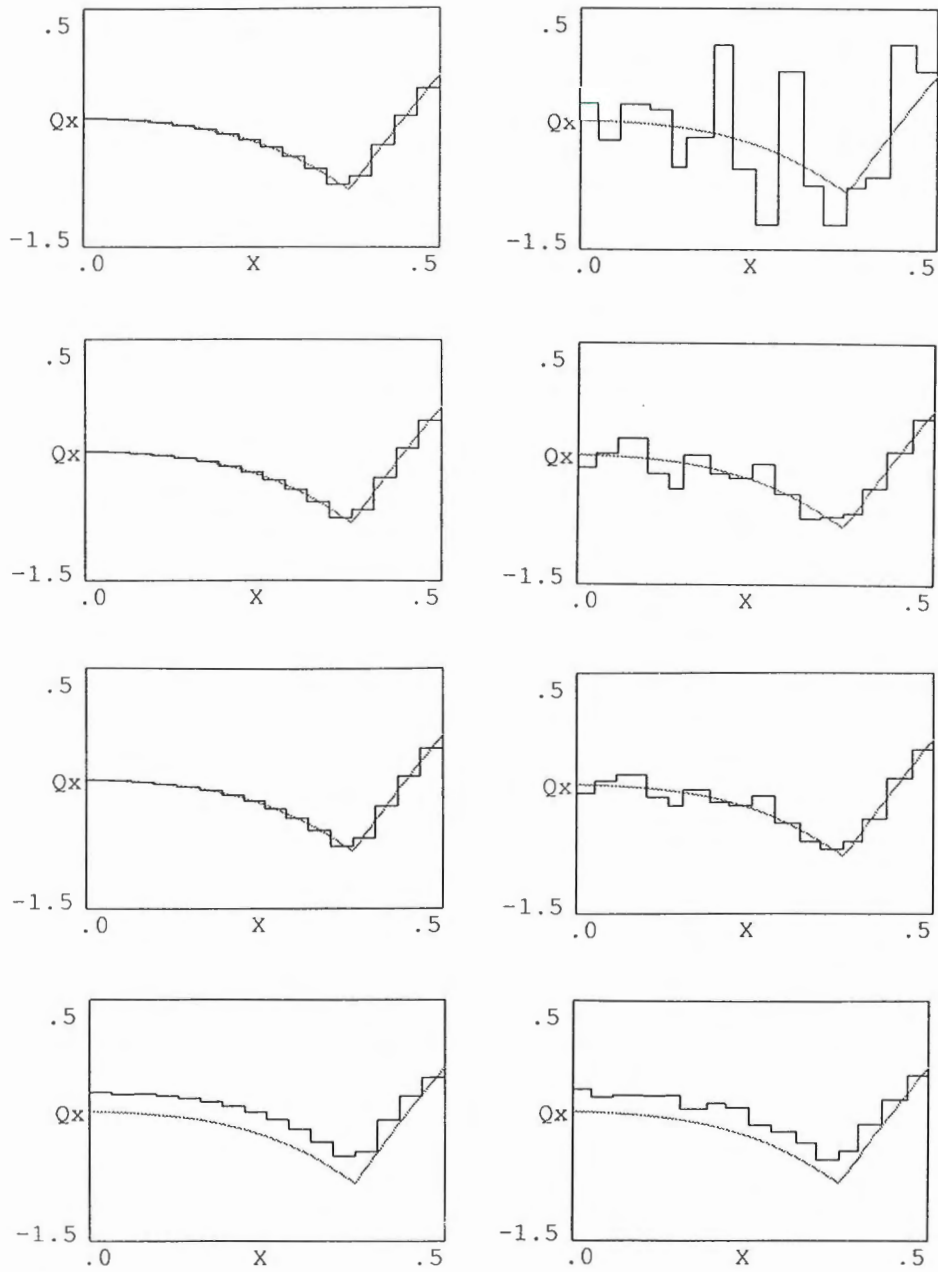
17

Figure 4: The distribution of the shear force Q_x along the horisontal symmetry line for the SRI (top), the MITC4 (upper middle), the STAB4 (lower middle) and the STAB3 (bottom). A regular (left) and irregular (right) mesh with $N = 16$. The thickness of the plate is $t = 0.01$. The dotted line gives the exact solution.

18

are as in Figure 4. The shear for the SRI with the irregular mesh is so highly oscillating that there is not any point in showing it. For the regular mesh the SRI gives a shear which is very near that of the MITC4.

Table 9. The normalized centerpoint deflections $w_{FE}(\text{center})/w(\text{center})$ for the regular and irregular meshes with $t = 0.001$. Three noded elements.

	STAB3		HT		HTRI	
N	Regular	Irregular	Regular	Irregular	Regular	Irregular
4	0.9661	0.9639	0.0327	0.0377	0.3868	0.3685
8	0.9916	0.9907	0.3496	0.4058	0.9268	0.9246
16	0.9980	0.9977	0.8824	0.8968	0.9927	0.9910

Table 10. The normalized centerpoint deflections $w_{FE}(\text{center})/w(\text{center})$ for the regular and irregular meshes with $t = 0.001$. Four noded elements.

	STAB4		MITC4		SRI	
N	Regular	Irregular	Regular	Irregular	Regular	Irregular
4	1.0005	1.0005	0.9750	0.9775	0.9750	0.9344
8	1.0004	1.0004	0.9942	0.9931	0.9942	0.8001
16	1.0001	1.0001	0.9986	0.9983	0.9986	0.8434

Table 11. The L_2-errors $\|w - w_{FE}\|_{L_2}/\|w\|_{L_2}$ for the regular and irregular meshes with $t = 0.001$. Three noded elements.

	STAB3		HT		HTRI		INT	
N	Regular	Irregular	Regular	Irregular	Regular	Irregular	Regular	Irregular
4	0.0509	0.0530	0.9663	0.9609	0.6032	0.6239	0.0249	0.0260
8	0.0130	0.0141	0.6445	0.5880	0.0757	0.0756	0.0063	0.0070
16	0.0032	0.0035	0.1210	0.1061	0.0083	0.0099	0.0016	0.0017

Table 12. The L_2-errors $\|w - w_{FE}\|_{L_2}/\|w\|_{L_2}$ for the regular and irregular meshes with $t = 0.001$. Four noded elements.

	STAB4		MITC4		SRI		INT	
N	Regular	Irregular	Regular	Irregular	Regular	Irregular	Regular	Irregular
4	0.0213	0.0195	0.0377	0.0371	0.0377	0.0838	0.0274	0.0274
8	0.0054	0.0061	0.0095	0.0109	0.0095	0.2241	0.0069	0.0077
16	0.0013	0.0015	0.0024	0.0027	0.0024	0.1784	0.0017	0.0019

Table 13. The L_2-errors $\|M - M_{FE}\|_{L_2}/\|M\|_{L_2}$ for the regular and irregular meshes with $t = 0.001$. Three noded elements.

N	STAB3		HT		HTRI		INT	
	Regular	Irregular	Regular	Irregular	Regular	Irregular	Regular	Irregular
4	0.1997	0.2054	0.9669	0.9619	0.6413	0.6681	0.1923	0.1968
8	0.0987	0.1004	0.6591	0.6186	0.1610	0.1696	0.0975	0.0991
16	0.0492	0.0504	0.1425	0.1442	0.0553	0.0656	0.0490	0.0502

Table 14. The L_2-errors $\|M - M_{FE}\|_{L_2}/\|M\|_{L_2}$ for the regular and irregular meshes with $t = 0.001$. Four noded elements.

N	STAB4		MITC4		SRI		INT	
	Regular	Irregular	Regular	Irregular	Regular	Irregular	Regular	Irregular
4	0.1186	0.1188	0.1187	0.1192	0.1187	0.2183	0.1137	0.1155
8	0.0587	0.0632	0.0587	0.0640	0.0587	0.4221	0.0581	0.0623
16	0.0293	0.0314	0.0293	0.0317	0.0293	0.3626	0.0292	0.0313

Table 15. The L_2-errors $\|Q - Q_{FE}\|_{L_2}/\|Q\|_{L_2}$ for the regular and irregular meshes with $t = 0.001$. Three noded elements.

N	STAB3		HT		HTRI	
	Regular	Irregular	Regular	Irregular	Regular	Irregular
4	0.4294	0.4363	65.079	69.372	158.98	151.75
8	0.3791	0.3911	169.56	166.86	71.721	69.868
16	0.3621	0.3763	114.92	105.41	18.017	19.263

Table 16. The L_2-errors $\|Q - Q_{FE}\|_{L_2}/\|Q\|_{L_2}$ for the regular and irregular meshes with $t = 0.001$. Four noded elements.

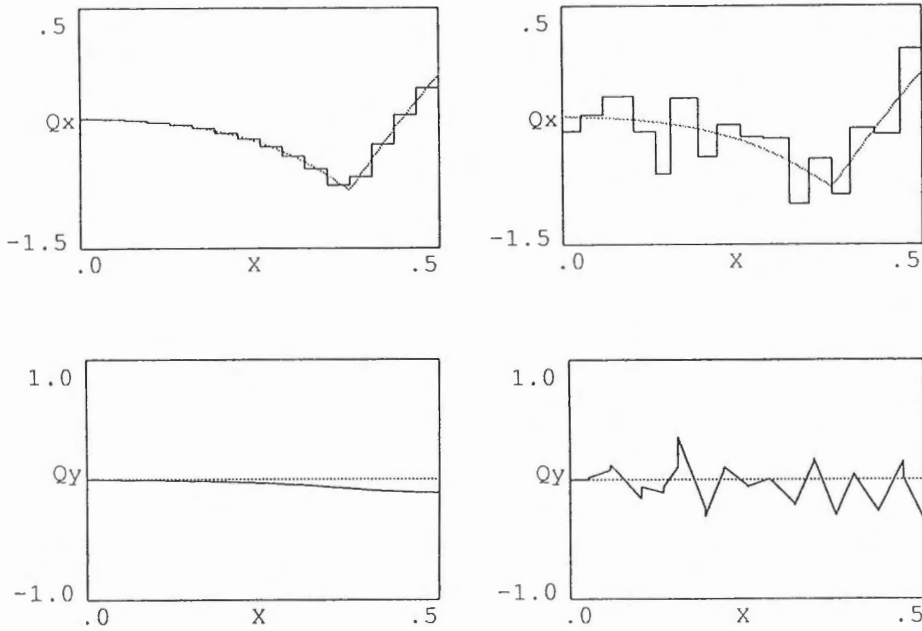| N	STAB4		MITC4		SRI	
	Regular	Irregular	Regular	Irregular	Regular	Irregular
4	0.2493	0.2744	0.2497	0.3053	0.2806	4.5754
8	0.1239	0.1733	0.1240	0.3080	0.1431	25.050
16	0.0610	0.1426	0.0610	0.2644	0.0713	48.855

Figure 5: The distribution of the shear forces Q_x and Q_y along the horisontal symmetry line for the MITC4 with a regular (left) and irregular (right) mesh with $N = 16$. The thickness of the plate is $t = 0.001$. The dotted line gives the exact solution.

The dependence of the accuracy of the stabilized elements on the parameter α

The accuracy of the stabilized HT and MITC4 elements clearly depends on the choice of the numerical parameter α. We will next study this dependence and we choose the previous test example with irregular mesh, $N = 8$ and $t = 0.01$. Figures 6 - 10 show the normalized centerpoint deflection, and the L_2-errors for the deflection, bending moment and shear force with respect to the parameter α.

As we can see from Figures 6 and 7, a larger α gives a "more flexible" plate. The accuracy of the deflection is (in this case) optimal if we choose $\alpha \approx 0.2$ for the stabilized MITC4 and $\alpha \approx 0.4$ for the stabilized HT. From Figure 8 we find that the normalized L_2-error in the bending moment is almost a constant with respect to α. Figures 9 and 10 give the normalized L_2-errors in shear force. As we can see, a larger α increases the accuracy of the shear.

The question of which would be the best value of the alpha is not properly posed. It depends on what quantity one is interested in and in the error measure.
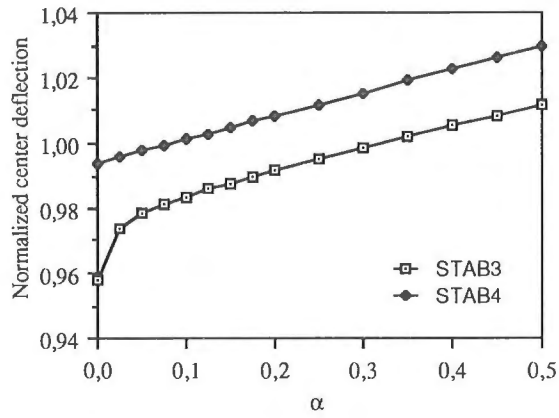
Figure 6: The normalized centerpoint deflection $w_{FE}(\text{center})/w(\text{center})$ with respect to the parameter α.
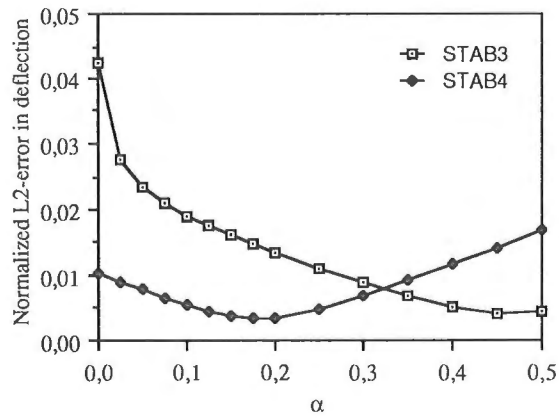

Figure 7: The errors $\|w - w_{FE}\|_{L_2}/\|w\|_{L_2}$ with respect to the parameter α.
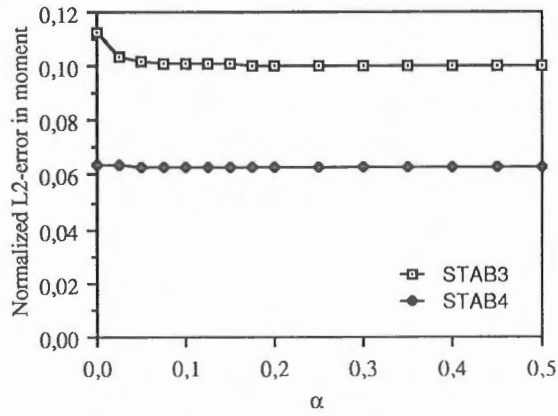
22

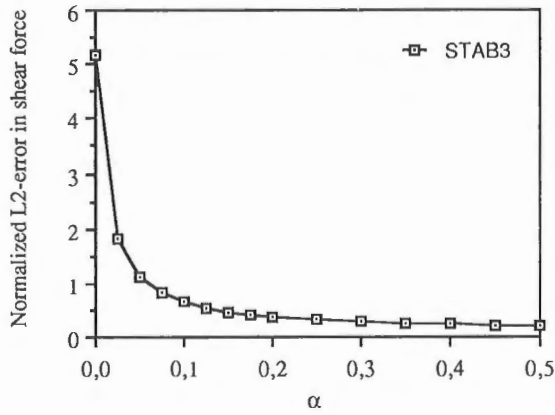Figure 8: The errors $\|M - M_{FE}\|_{L_2}/\|M\|_{L_2}$ with respect to the parameter α.

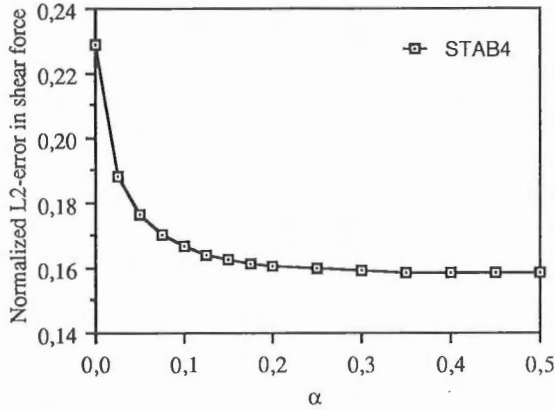Figure 9: The error $\|Q - Q_{FE}\|_{L_2}/\|Q\|_{L_2}$ with respect to the parameter α.

23

Figure 10: The error $\|Q - Q_{FE}\|_{L_2}/\|Q\|_{L_2}$ with respect to the parameter α.

Furthermore, it also depends, for example, on the boundary conditions and the geometry of the plate, cf. [24]. What is more important to note is that the accuracy does not seem to be very sensitive to the choice. Note also that the stabilized HT is more sensitive than the stabilized MITC4. The probable explanation to this is that the unstabilized MITC4 have already some intrinsic stability, it mostly works quite well. The same conclusion can be drawn from the choice of boundary conditions. From a stability point of view the hard clamped condition is the worst case and for this the sensitivity with respect to α is greatest, cf. [24, Figure 15].

In practice, the choice given in previous section has proven to work well in all our benchmark examples as well as in some real life calculations.

The Weissman-Taylor robustness test

We finally consider a rather simple coarse mesh distortion sensitivity test introduced by Weissman and Taylor [30]. One symmetric quarter of a hard clamped square plate is divided into a 2×2 mesh as shown in Figure 11. The middle node is then moved along the the cross diagonal direction from the top left to the bottom right corner so that the mesh becomes distorted. The plate is subject to a constant pressure load and the thickness of the plate is $t = 0.01$.

Figures 12 - 15 show the normalized centerpoint deflections and the L_2-errors in deflection, bending moment and shear force for the original MITC4, SRI and for the stabilized modifications of the HT and MITC4 elements as a function of the movement δ. The reason for not taking the original HT nor its modified version with selective reduced integration into consideration here is that these elements lock severely in this test.
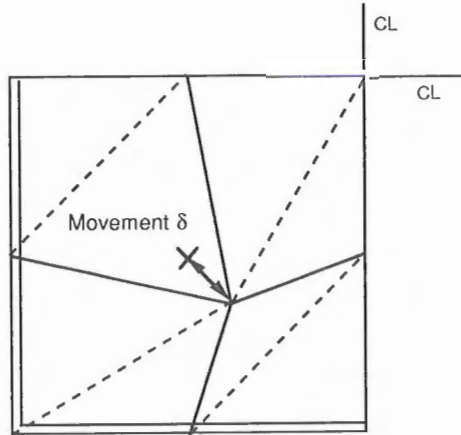
Figure 11: One symmetric quarter of the clamped square plate used in the Weiss-man-Taylor robustness check. The clamped plate is subject to a constant pressure load.
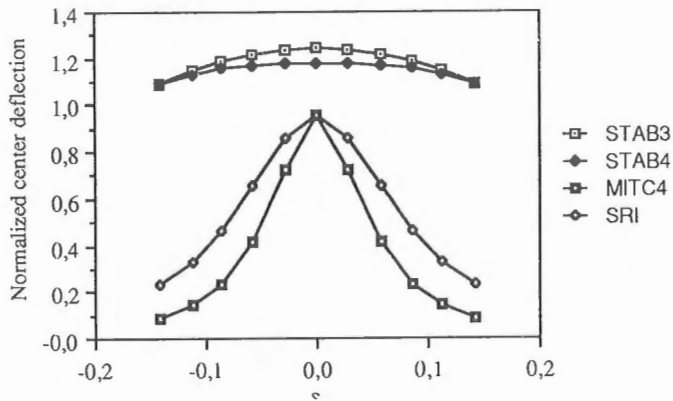

Figure 12: The distortion sensitivity of $w_{FE}(\text{center})/w(\text{center})$ for the 2×2 mesh.
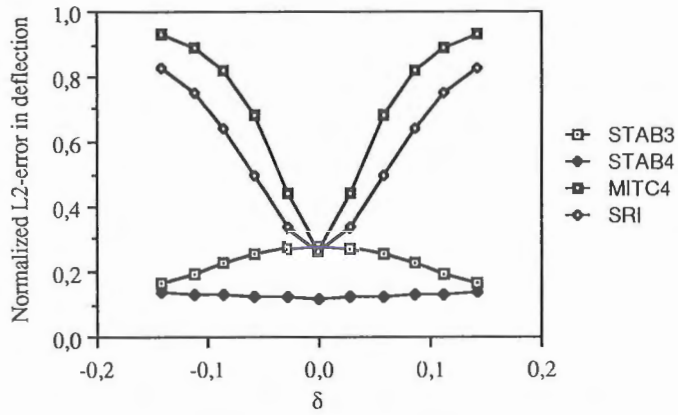
25

Figure 13: The distortion sensitivity of the errors $||w - w_{FE}||_{L_2}/||w||_{L_2}$ for the 2×2 mesh.
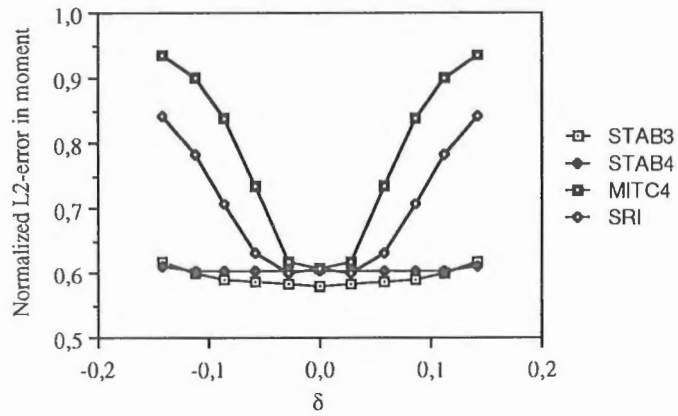

Figure 14: The distortion sensitivity of the errors $||M - M_{FE}||_{L_2}/||M||_{L_2}$ for the 2×2 mesh.
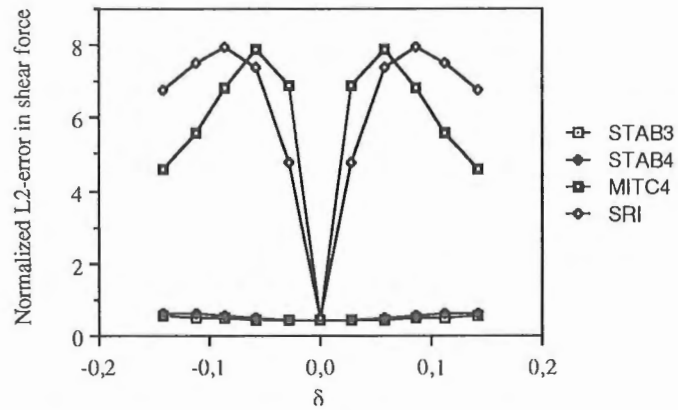

Figure 15: The distortion sensitivity of the errors $||Q - Q_{FE}||_{L_2}/||Q||_{L_2}$ for the 2×2 mesh.

As we can see from the figures, the stabilized elements are much more robust than the others. Especially the shear force of the original MITC4 and SRI elements is very sensitive for even small changes in δ.

Conclusions

In this paper we have presented stable and optimally convergent three and four noded Reissner-Mindlin plate elements. By performing some quite extensive numerical tests we have showed that the new elements perform very well and better than some methods which are well known in the literature. This confers the results of the mathematical analysis of the methods.

We have tried to do as revealing "benchmark" computations as possible. In the literature this aspect is far too often treated in a non-satisfactory way. A typical example would be to calculate a square unit plate with a uniform load and a regular mesh, and to report on, say, the centerpoint deflection and the maximum moments. By such a simple test one could, e.g., draw the conclusion that the method with selective reduced integration is a good method. Our results show, however, that the method is more or less useless. Instead, we think that in test calculations one should report on all quantities of physical interest for different meshes and loadings, etc. By doing this we have shown that the possible non-stability of a method is first seen in an inaccurate and oscillating shear force. That the shear force is a critical variable appears to be well known (see the remark on page 224 of [20]), but usually the results for it are not reported. To our knowledge, this problem has not been addressed until quite recently [23].

To find good benchmark tests is, however, far from a trivial task. We refer to [6, 4, 5] for some recent interesting discussions on this.

References

[1] D.N. Arnold and R.S. Falk. Edge effects in the Reissner-Mindlin plate theory. In A.K. Noor, T. Belytschko, and J.C. Simo, editors, *Analytical and Computational Models of Shells.*, pages 71–89, New York, 1989. ASME.

[2] D.N. Arnold and R.S. Falk. A uniformly accurate finite element method for the Reissner-Mindlin plate. *SIAM J. Num. Anal.*, 26:1276–1290, 1989.

[3] D.N. Arnold and R.S. Falk. Asymptotic analysis of the boundary layer for the Reissner-Mindlin plate model. To appear in SIAM J. Math. Anal.

[4] I. Babuška. The problem of modelling the elastomechanics in engineering. *Comp. Meths. Appl. Mech. Engrg*, 82:155–182, 1990.

27

[5] I. Babuška and J.T. Oden. Benchmark computation: what is the purpose and meaning? *IACM Bulletin*, 7(4):83–84, 1992.

[6] I. Babuška and T. Scapallo. Benchmark computations and performance evaluation for a rhombic plate bending problem. *Int. J. Num. Meths. Engng.*, 28:155–179, 1989.

[7] K.J. Bathe and F. Brezzi. On the convergence of a four node plate bending element based on Reissner-Mindlin theory. In J. R. Whiteman, editor, *The Mathematics of Finite Elements and Applications V. MAFELAP 1984*, pages 491–503. Academic Press, 1985.

[8] K.J. Bathe and F. Brezzi. A simpified analysis of two plate bending elements - the MITC4 and MITC9 elements. In G.N. Pande and J. Middleton, editors, *NUMETA 87, Vol. 1, Numerical Techniques for Engineering Analysis and Design*. Martinus Nijhoff Publishers, 1987.

[9] K.J. Bathe, F. Brezzi, and S.W. Cho. The MITC7 and MITC9 plate elements. *Comput. Struct.*, 32:797–814, 1989.

[10] K.J. Bathe, M.L. Bucalem, and F. Brezzi. Displacement and stress convergence of our MITC plate bending elements. *Eng. Comput.*, 7:291–302, 1990.

[11] K.J. Bathe and E. Dvorkin. A four node plate bending element based on Mindlin-Reissner plate theory and mixed interpolation. *Int. J. Num. Meths. Eng.*, 21:367–383, 1985.

[12] J.-L. Batoz and G. Dhatt. *Modélisation des Structures par Element Finis, Vol. 2. Poutres et Plaques*. Hermès, Paris, 1990.

[13] F. Brezzi, M. Fortin, and R. Stenberg. Error analysis of mixed-interpolated elements for Reissner-Mindlin plates. *Mathematical Models and Methods in Applied Sciences*, 1:125–151, 1991.

[14] R.D. Cook, D.S. Malkus, and M.E. Plesha. *Concepts and Applications of Finite Element Analysis*. John Wiley, 3 edition, 1989.

[15] R. Durán and E. Liberman. On mixed finite element methods for the Reissner-Mindlin plate model. *Math. of Comp*, 58(198):561–573, 1992.

[16] L. Franca, R. Stenberg, and T. Vihinen. A nonconforming linear element for Reissner-Mindlin plates. In *The Proceedings of the 13th IMACS World Congress on Computational and Applied Mathematics. Vol. 4. Trinity College, Dublin, Ireland*, pages 1907–1908, 1991.

[17] L.P. Franca and R. Stenberg. A modification of a low-order Reissner-Mindlin plate bending element. In J. R. Whiteman, editor, *The Mathematics of Finite Elements and Applications VII. MAFELAP 1990*, pages 425–436. Academic Press, 1991.

[18] I. Fried and S.K. Yang. Triangular, nine-degrees-of-freedom, C^0 plate bending element of quadratic accuracy. *Quart. Appl. Math.*, 31:303–312, 1973.

[19] T.J.R. Hughes. *The Finite Element Method. Linear Static and Dynamic Analysis*. Prentice-Hall, 1987.

[20] T.J.R. Hughes and L.P. Franca. A mixed finite element formulation for Reissner-Mindlin plate theory: Uniform convergence of all higher-order spaces. *Comp. Meths. Appl. Mech. Engrg.*, 67:223–240, 1988.

[21] T.J.R. Hughes and R. L. Taylor. The linear triangular plate bending element. In J. R. Whiteman, editor, *The Mathematics of Finite Elements and Applications IV. MAFELAP 1981*, pages 127–142. Academic Press, 1982.

[22] C. Johnson and J. Pitkäranta. Analysis of some mixed finite element methods related to reduced integration. *Math. Comput.*, 38:375–400, 1982.

[23] D. Lasry and T. Belytschko. Transverse shear oscillations in four-node quadrilateral plate elements. *Computers and Structures*, 27:393–398, 1987.

[24] M. Lyly, R. Stenberg, and T. Vihinen. A stable bilinear element for Reissner-Mindlin plate model. *Comp. Meths. in Appl. Mech. Engrg.*, 110:343–357, 1993.

[25] M. Mikkola. *Levyjen, Laattojen ja Kuorien Teoriaa*. Otakustantamo, 1986.

[26] J. Pitkäranta. Analysis of some low-order finite element schemes for Mindlin-Reissner and Kirchhoff plates. *Numer. Math.*, 53:237–254, 1988.

[27] J. Pitkäranta and R. Stenberg. Error bounds for the approximation of Stokes problem with bilinear/constant elements on irregular quadrilateral meshes. In J. R. Whiteman, editor, *The Mathematics of Finite Elements and Applications V. MAFELAP 1984*, pages 325–334. Academic Press, 1985.

[28] R. Stenberg. A new finite element formulation for the plate bending problem. Helsinki University of Technology, Laboratory for Strength of Materials. Report 17, 1993. To be published in L. Trabucho, editor, *Proceedings of the International Conference on Asymptotic Methods for Elastic Structures. Lisbon, October 4-8, 1993*.

[29] R. Stenberg and T. Vihinen. Calculations with some linear elements for Reissner-Mindlin plates. In P. Ladeveze and O.C. Zienkiewicz, editors, *Proceedings of the European Conference on New Advances in Computational Structural Mechanics*, pages 505–511, 1991.

[30] S. Weissman and R. Taylor. Resultant fields for mixed plate bending elements. *Comp. Meths. Appl. Mech. Engrg.*, 79:321–355, 1990.

[31] O.C. Zienkiewicz and R.L. Taylor. *The Finite Element Method, 4th edition. Vol I, Basic Formulation and Linear Problems*. MacGraw-Hill, 1989.

[32] O.C. Zienkiewicz and R.L. Taylor. *The Finite Element Method, 4th edition, Vol II, Solid and Fluid Mechanics, Dynamics and Non-linearity*. MacGraw-Hill, 1991.

Mikko Lyly, M.Sc. (Eng.), Rolf Stenberg, Docent
Laboratory for Strength of Materials
Helsinki University of Technology